SUPPORTING INFORMATION

Chiral Microneedles from an achiral Bis(BODIPY): Spontaneous Mirror Symmetry Breaking Leading to a Promising Photoluminescent Organic Material

Leire Gartzia-Rivero,[†] César Ray Leiva,[‡] Esther M. Sánchez-Carnerero,[‖] Jorge Bañuelos,*[†] Florencio Moreno,[‡] Beatriz L. Maroto,[‡] Inmaculada García Moreno,[§] Lourdes Infantes,[¥] Bianchi Mendez,[⊥] Iñigo López Arbeloa,[†] and Santiago de la Moya*[,‡]

[†]Dpto. Química Física, Universidad del País Vasco (UPV/EHU), 644, 48080 Bilbao, Spain.

[‡]Dpto. Química Orgánica, Universidad Complutense de Madrid, Ciudad Universitaria s/n, 28040 Madrid, Spain.

[‖]Dpt. of Chemistry and RECETOX, Masaryk University, Kamenice 5, 62500 Brno, Czech Republic.

[§]Dpto. de Sistemas de Baja Dimensionalidad, Superficies y Materia Condensada, Instituto de Química Física Rocasolano, CSIC, Serrano 119, 28006 Madrid, Spain.

[¥]Dpto. de Cristalografía y Biología Estructural, Instituto de Química Física Rocasolano, CSIC, Serrano 119, 28006 Madrid, Spain

[⊥]Dpto. de Física de Materiales, Universidad Complutense de Madrid, Ciudad Universitaria s/n, 28040 Madrid, Spain.

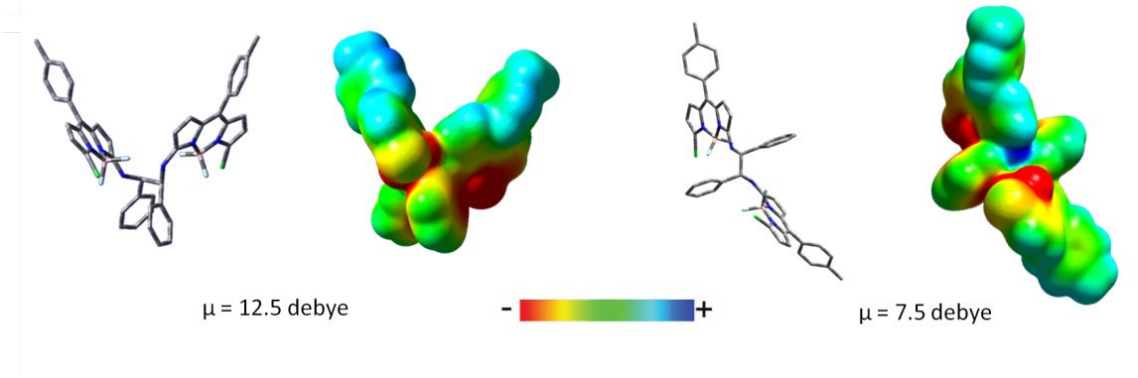

Figure S1. Computed preferred conformations and corresponding electron-density maps and permanent dipolar moments in $CHCl_3$ (B3LYP/6-31+G*) for *meso* **1** (left) and its chiral (*R,R*) stereoisomer (right). Note that achiral **1** adopts a pleated conformation, whereas its chiral diastereomer adopts an axially-chiral conformation with a preferred (*M*) helical configuration.

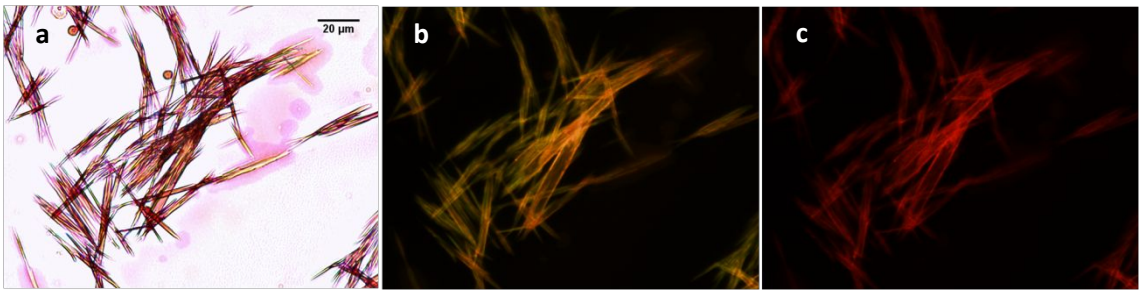

Figure S2. Transmission (a) and fluorescence images (b and c) of representative **1** needles under excitation with band-pass filter of 470/40 nm and monitoring the emission with a cut-off filter of 515 nm (b) and 580 nm (c).

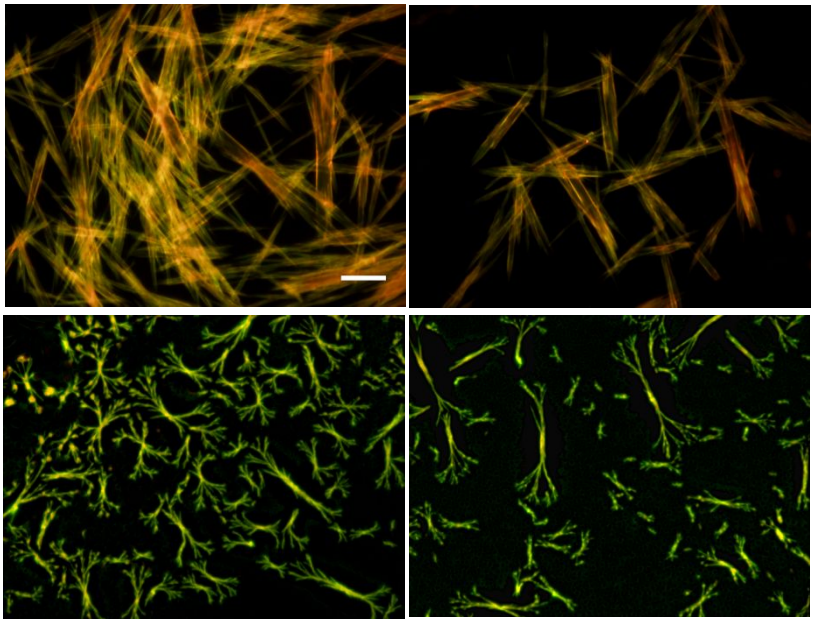

Figure S3. Fluorescence images of the two different morphologies detected for **1:** major totally-ripened crystalline needles obtained at higher dye concentrations (top); wires-enrolling fibers obtained at lower dye concentrations (bottom). Band-pass filter of 470/40 nm for the excitation; cut-off filter of 515 nm for recording the emission. 20-μm Scale-bar.

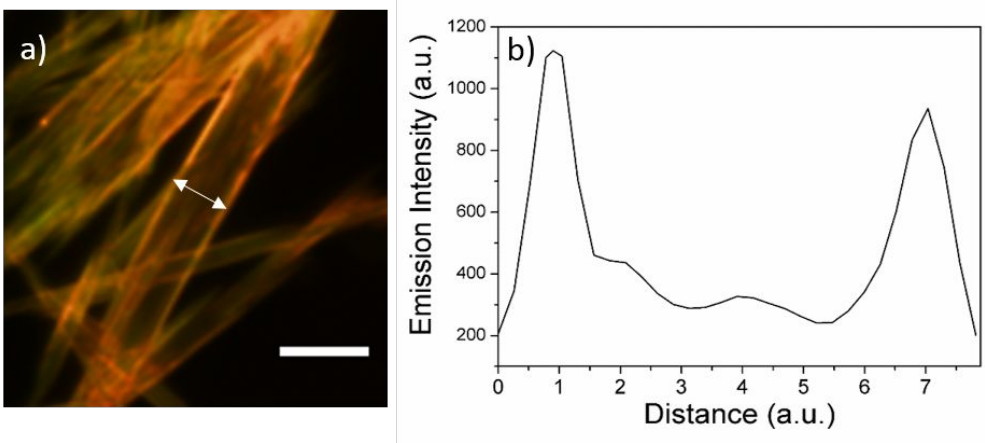

Figure S4. Fluorescence image of **1** needles showing energy migration towards the needle edges (a; 10-μm scale-bar) and emission-intensity profile across the width of a single needle (b).

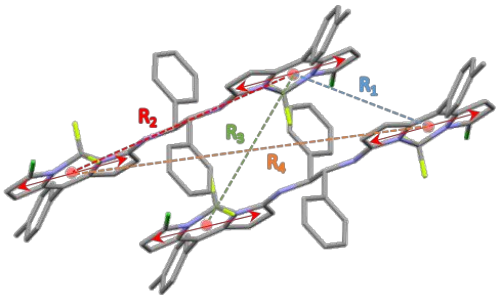

	R1	R2	R3	R4
Distance (Å)	7,2	11,1	9,4	16,1
α (°)	0	0	0	0
Θ (°)	28,7	41,2	77,4	25,0
Δν (cm^{-1})	-509,1	-87,2	+100,6	-48,6

Figure S5. Calculated energy-splitting values (Δν; Davydov splitting) from possible dipole couplings (R1-R4) between nearest neighbor dipyrrins in the crystal structure obtained by X-Ray diffraction (key distances and angles are also given). Red double-head arrow show the transition dipole moment (along the longitudinal axis of the dipyrrin).

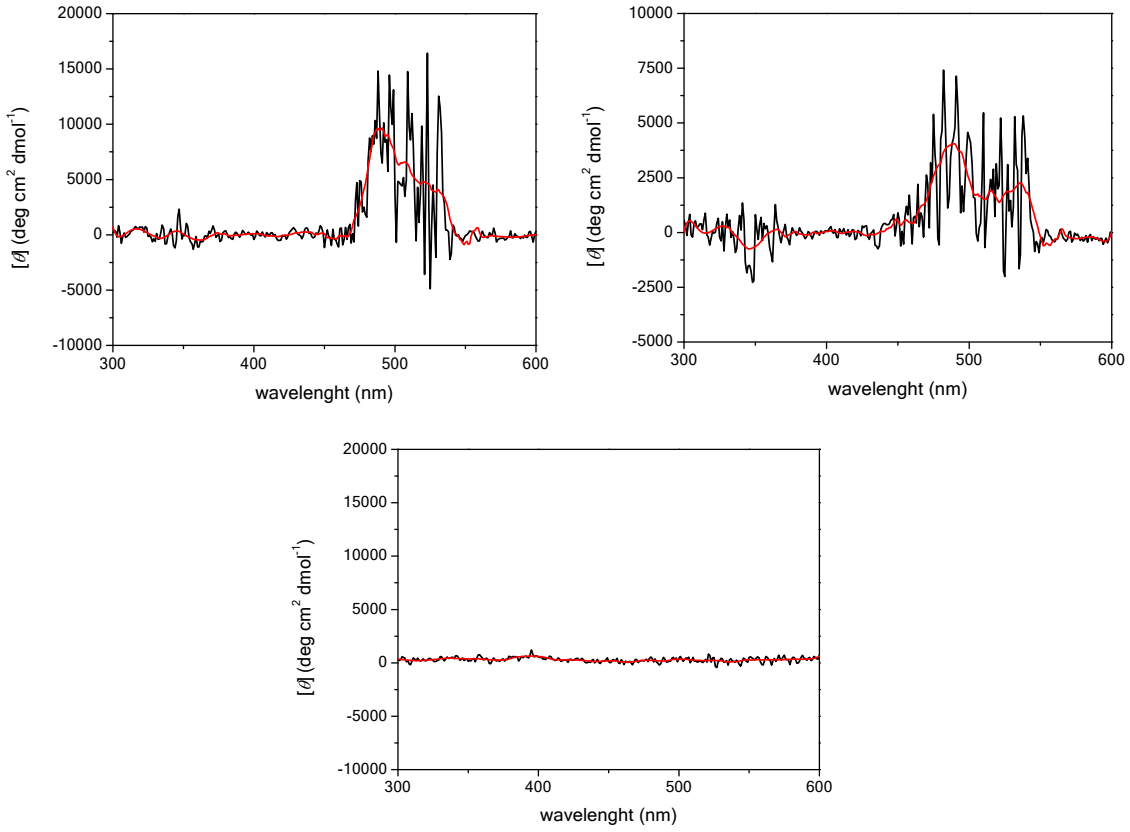

Figure S6. Examples of positive ECD spectra recorded from **1** needles dispersed in $CHCl_3$ at 1.4 10^{-4} M (top, left) and $6.9 \cdot 10^{-5}$ M (top, right), and silent ECD spectra observed for individual **1** molecules at $6.9 \cdot 10^{-6}$ M (bottom). Formations of chiral nanostructured fibers is detected at high enough concentrations (top) by switching on the silent ECD (bottom) observed at a low enough concentration (disaggregated state). Red line indicates the estimated smoothed spectrum from the corresponding recorded (black line) spectrum.